Vehicle System Dynamics: International Journal of Vehicle Mechanics and Mobility

Publication details, including instructions for authors and subscription information:
http://www.tandfonline.com/loi/nvsd20

THE MAGIC FORMULA TYRE MODEL

Hans B. Pacejka [a] & Egbert Bakker [b]

[a] Delft University of Technology, Delft, the Netherlands

[b] NedCar Engineering & Development B.V., Helmond, the Netherlands

Version of record first published: 06 Aug 2007.

To cite this article: Hans B. Pacejka & Egbert Bakker (1992): THE MAGIC FORMULA TYRE MODEL, Vehicle System Dynamics: International Journal of Vehicle Mechanics and Mobility, 21:S1, 1-18

To link to this article: http://dx.doi.org/10.1080/00423119208969994

THE MAGIC FORMULA TYRE MODEL

Hans B. Pacejka[1] and Egbert Bakker[2]

1) Delft University of Technology Delft, the Netherlands
2) NedCar Engineering & Development B.V., Helmond, the Netherlands

SUMMARY

An account is given of the latest version 3 of the Magic Formula tyre model. The model provides a set of mathematical formulae from which the forces and moment acting from road to tyre can be calculated at longitudinal, lateral and camber slip conditions, which may occur simultaneously. The model aims at an accurate description of measured steady-state tyre behaviour. The coefficients of the basic formula represent typifying quantities of the tyre characteristic. By selecting proper values, the characteristics for either side force, aligning torque or fore and aft force can be obtained. The new version of the model contains physically based formulations to avoid the introduction of correction factors. Double-sided, possibly non-symmetric pure slip curves are employed as the basis for combined slip calculations. Suggestions are given to estimate the driving part of the longitudinal slip curve and to represent the characteristic at rolling backwards.

INTRODUCTION

In the literature (cf.[1]) a considerable number of models of tyre force and moment generating properties have been described. These models have been developed for use in vehicle dynamics studies. Some of these models are based on the physical nature of the tyre. Other models are basically empirical. Almost all models which aim at a more or less accurate description of measured characteristics rely on partly empirical formulations.

Relatively recently, an empirical tyre model, which is partly based on physical insight into tyre force generating properties, has been developed [2] and subsequently enhanced and improved. The work was done in a cooperative effort by the Delft University of Technology and Volvo Car Corporation. The model is capable of accurately describing

steady-state tyre force and moment characteristics for use in vehicle dynamics simulation studies. The heart of the model is formed by the formula which has become known under the name "Magic Formula". The formula is capable of producing force and moment characteristics at pure slip conditions, i.e. at either pure cornering (possiby including camber) or pure braking or driving.

For the description of force and moment at combined slip conditions (e.g. at braking in a curve) the model provides for an extension which in a proper way combines the formulae for pure slip conditions. In the next section, the paper gives an elaborate treatment of the properties of the formula. The subsequent section deals with the extension for combined slip.

The use of the model as well as the fitting procedures and the accuracy achieved have treated and illustrated in the accompanying papers [3,4] published in the same issue.

THE MAGIC FORMULA FOR PURE SLIP

For the simple case of pure side or pure longitudinal slip the "Magic Formula" can be employed. The formula expresses the sideforce F_y, the aligning torque M_z and the longitudinal force F_x as a function of the side slip angle α and the longitudinal slip κ respectively. The general form of the formula which holds for a given value of vertical load and camber angle reads:

$$y(x) = D \sin [C \arctan \{Bx - E(Bx - \arctan(Bx))\}] \qquad (1)$$

where

$$Y(X) = y(x) + S_v$$
$$x = X + S_h$$

The Magic Formula $y(x)$ typically produces a curve which passes through the origin $x = y = 0$, reaches a maximum and subsequently tends to a horizontal asymptote. For constant coefficients B,C,D and E the curve exhibits an anti-symmetric shape with respect to the origin. To allow the curve to show an offset with respect to the origin, the shifted coordinate system $Y(X)$ is introduced.

The formula is capable of producing characteristics which closely match measured curves for the side force F_y, the aligning torque M_z and the longitudinal force F_x as functions of their respective slip quantities: the slip angle α and the longitudinal slip κ. The output variable Y stands for either F_y, M_z or F_x and the input X may represent α or κ.

Figure 1 illustrates the meaning of some of the coefficients with the help of a typical side force characteristic. The offsets S_h and S_v appear to occur when ply steer and conicity effects cause the F_y and M_z curves not to pass through the origin. Similarly, the rolling resistance gives rise to the offset of the F_x characteristic. Also, the camber angle γ may give rise to a considerable offset in the F_y vs α diagram which is accompanied by an appreciable deviation from the

purely anti-symmetric shape. An adapted version of the formula allows the calculated curves to show a more precise shape in the presence of camber. Also the difference in shape which is expected to occur between F_x curves in the braking and in the driving ranges can be taken care of.

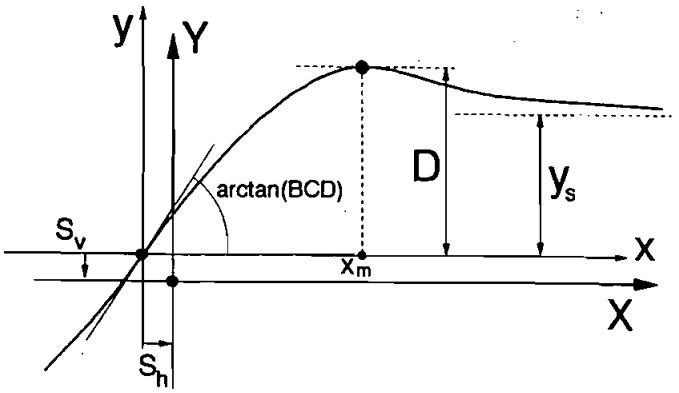

Fig. 1. A typical tyre characteristic indicating the meaning of some of the coefficients of formula (1).

Obviously, coefficient D represents the peak value (with respect to the x-axis) and the product BCD corresponds to the slope at the origin ($x = y = 0$). The factor C controls the limits of the range of the argument of the sine function. It thereby determines the shape of the resulting curve. Typical values of the shape factor C are: 1.3 for the side force, 2.4 for the aligning torque and 1.65 for the brake force characteristic. The factor B is left to control to slope at the origin and is therefore called the stiffness factor. The remaining factor E appears to be necessary to influence the curvature near the peak of the curve. At the same time E controls the slip x_m at which the peak occurs (if present).

$$E = \frac{Bx_m - \tan(\frac{\pi}{2C})}{Bx_m - \arctan(Bx_m)} \tag{2}$$

The asymptotic value which y approaches at large slip values equals

$$y_s = D \sin(\frac{\pi}{2}C) \tag{3}$$

From these expressions the initial values for C and E may be obtained for the least square regression procedure to acquire an optimal match to measured data. More often, C is given a fixed value, typical for the kind of curve.

Figure 2 is presented to illustrate the quantitative role of the shape factor C and the curvature factor E. Since the influences of the peak factor D and the product BCD (the slope at $x = 0$) are obvious,

the diagrams of Fig. 2 have been made non-dimensional by using the ordinate y/D and the abscissa BCx. The shifts are disregarded. The resulting curves exhibit a slope and a maximum both equal to unity. By studying these diagrams one might be able to roughly fit a curve manually. An important aspect is, that E should not be given values larger than unity since for $E > 1$ the curve will not reach the maximum $y = D$ which is supposed to occur for $C > 1$.

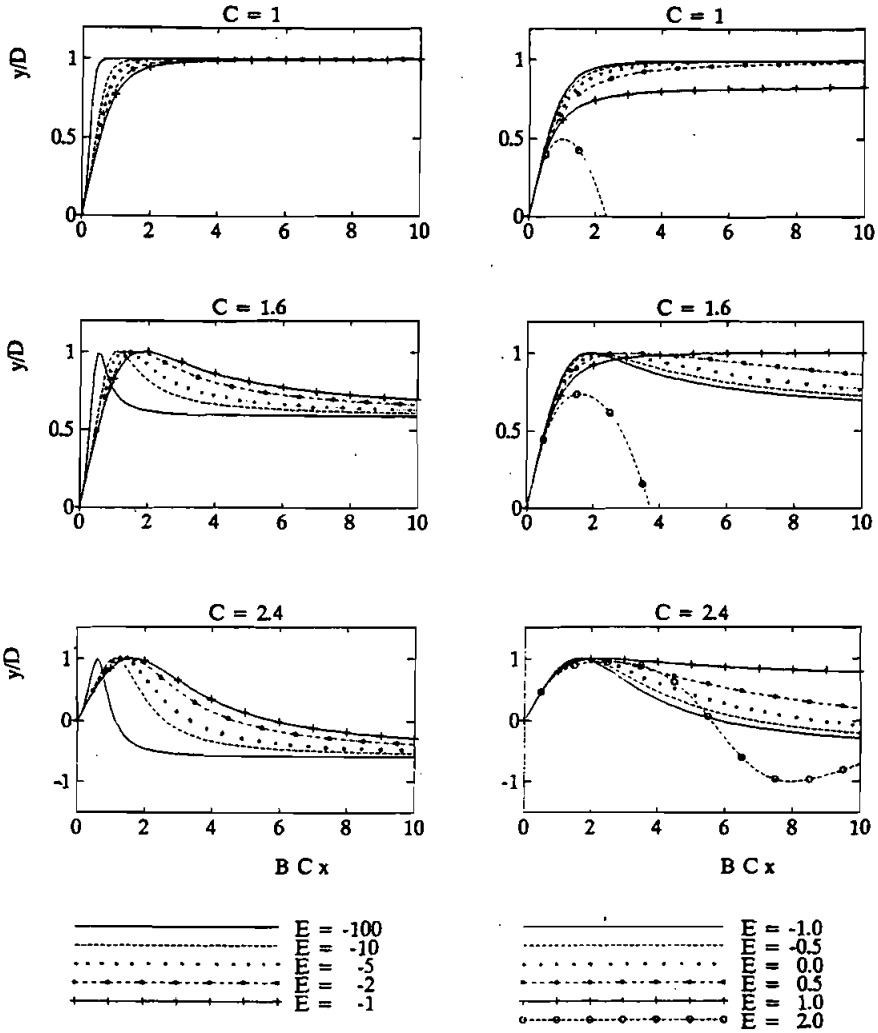

Fig. 2. Influence of the shape and curvature factors C and E on the non-dimensional Magic Formula characteristic.

An interesting property of the formula is the fact that at the origin a local 'S'-shape may be created. This occurs for negative values of E below a critical value which appears to depend on C. The critical value of E is found by considering the third derivative of the curve at the origin. With the use of the program DERIVE the following expression for the third derivative of $\bar{y} = y/D$ with respect to $\bar{x} = BCx$ at $x = 0$ has been obtained:

$$\frac{d^3\bar{y}}{d\bar{x}^3} = -\left(1 + 2\,\frac{E+1}{C^2}\right) \tag{4}$$

Obviously, the 'S'-shape arises at positive values of this expression, i.e. for

$$E < -(1 + \tfrac{1}{2}C^2) \tag{5}$$

Figure 2 illustrates that this phenomenon indeed occurs in the negative E range. This peculiar shape has been reported to occur sometimes in tyre characteristics, notably in the characteristic for the overturning couple M_x vs α. A successful fit of such a characteristic has been shown to be possible [5].

To represent curves showing different shapes (curvatures) in the left and right-hand side of the diagram, the curvature factor E may be made dependent on the sign of the abscissa (x):

$$E = E_o + \Delta E.\mathrm{sgn}(x) \tag{6}$$

As has been indicated in the Appendix, ΔE is represented by a function which provides for the important influence of the camber angle γ. Figure 3 depicts the asymmetry in shape which may occur typically in the presence of camber and in the complete F_x vs κ diagram (brake and drive slip). Of course, the asymmetry is achieved without effecting the continuity of the slope at the origin. The values for the slope BCD and for the peak value D remain the same.

For the offsets $S_{v,h}$ and the factors B,D and E, functions are provided to express their dependence on vertical load F_z and camber angle γ. The constants appearing in these functions are the ultimate parameters of the model.

The reader is referred to the Appendix for a complete set of formulae. For a proper distinction between formulae for F_x, F_y and M_z, subscripts x,y and z have been added to the variables and parameters of formula (1). It should be noted that, different from earlier publications, α is always expressed in radians, κ in units from -1 to + ∞ and F_z in Newtons. It is recommended to use different symbols for the parameters of formula (1) if alternative units are employed.

An interesting detail is the function for the cornering stiffness

$$BCD_y = a_3 \sin[2 \arctan(F_z/a_4)] \,.\, (1 - a_5|\gamma|) \tag{7}$$

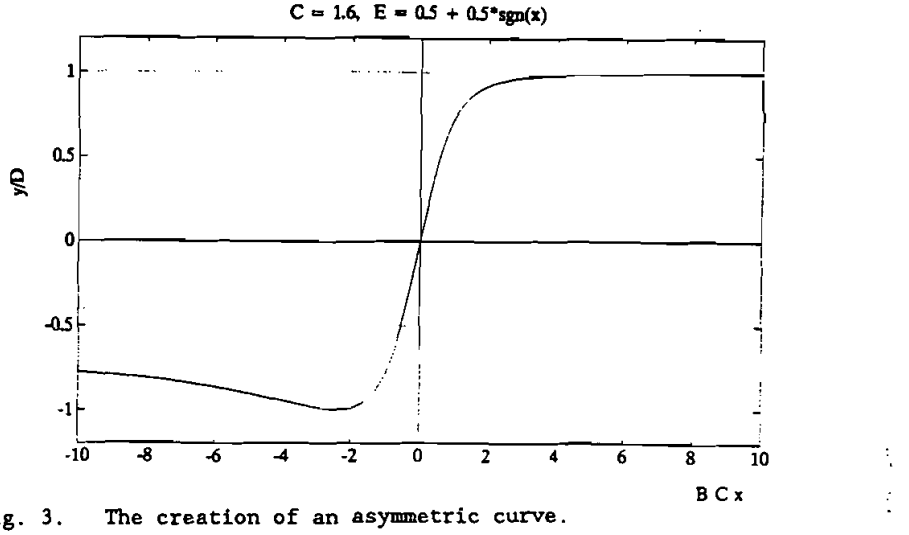

Fig. 3. The creation of an asymmetric curve.

For zero camber, the cornering stiffness attains a maximum a_3 at $F_z = a_4$. The slope at zero vertical load is $2a_3/a_4$. Figure 4 illustrates the relationship.

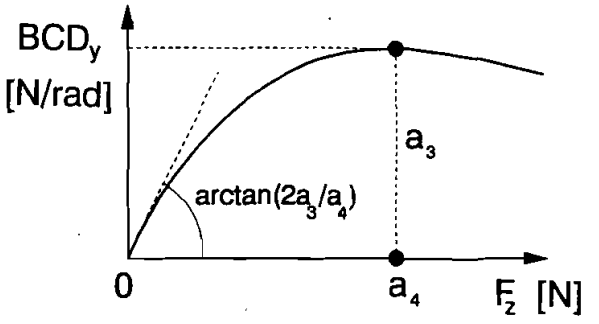

Fig. 4. The cornering stiffness as a function of vertical load according to expression (4) at zero camber.

THE FORMULA EXTENSION FOR COMBINED SLIP

The more complex case of combined slip requires the introduction of new slip quantities σ_x and σ_y. Figure 5 shows a top view of a tyre during combined cornering and braking. The force and torque acting on the tyre and the velocity of the wheel have been indicated:

* the total force with components in lateral and longitudinal directions (F_y and F_x),
* the self aligning torque (M_z),
* the speed in the direction of travel $\underline{V}$ which is composed of the slip speed vector ($\underline{V}_s$) and the rolling speed vector ($\underline{V}_r$) of the tyre ($V_r = V_x - V_{sx}$).

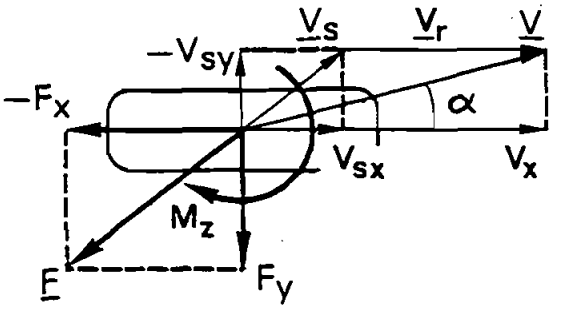

Fig. 5. Top view of tyre at combined braking and cornering, showing velocity and force vector diagrams.

The original practical slip quantities κ and α are defined as follows

$$\kappa = - V_{sx}/V_x \tag{8a}$$

$$\tan \alpha = - V_{sy}/V_x \tag{8b}$$

with V_{sx} and V_{sy} the components of the slip speed which may be defined as the velocity of point S. This point is thought to be attached to the rotating wheel body and, at the moment of observation, located below the wheel centre at a distance equal to the (free rolling) effective rolling radius r_e.

With Ω denoting the angular speed of rolling we define the linear speed of rolling

$$V_r = r_e \Omega \tag{9}$$

The theoretical slip quantities are defined as follows

$$\sigma_x = V_{sx}/V_r = - \frac{\kappa}{1 + \kappa} \tag{10a}$$

$$\sigma_y = V_{sy}/V_r = - \frac{\tan \alpha}{1 + \kappa} \tag{10b}$$

The magnitude of the theoretical slip vector is

$$\sigma = \sqrt{\sigma_x^2 + \sigma_y^2} \tag{10c}$$

The inverse relationships may also be of importance

$$\kappa = - \frac{\sigma_x}{1 + \sigma_x} \tag{11a}$$

$$\tan \alpha = - \frac{\sigma_y}{1 + \sigma_x} \tag{11b}$$

It should be kept in mind that these practical slip quantities are used as the arguments X_x and X_y in the functions for Y_x and Y_y respectively, according to the original formulae for pure slip (1).

A series of successive transformations and combinations are needed to arrive at the force components and the aligning torque which arise as a result of the combined slip.

First, both the F_x and F_y pure slip curves (possibly including camber) plotted as functions of σ_x and σ_y respectively are shifted horizontally to arrive at characteristics passing through the origins. The new abscissas, the components of the total theoretical composite slip σ_{tot}, become

$$\sigma_{xtot} = \sigma_x + \delta\sigma_x \tag{12a}$$

$$\sigma_{ytot} = \sigma_y + \delta\sigma_y \tag{12b}$$

with the horizontal shifts

$$\delta\sigma_x = - \frac{\delta\kappa}{1 - \delta\kappa} \tag{12c}$$

$$\delta\sigma_y = - \tan(\delta\alpha) \tag{12d}$$

At pure slip conditions ($\kappa = 0$ in (10b, 12b)) the total theoretical slip with components (12a,b) vanish at slip values $\kappa = -\delta\kappa$ and $\alpha = -\delta\alpha$ respectively.

The fact that finite values of slip ($-\delta\kappa$ and $-\delta\alpha$) are needed to make F_x and F_y equal to zero is a consequence of hysterisis and of the asymmetric construction of the tyre (ply-steer, conicity). If the wheel rolls at a camber angle, a relatively large slip angle $-\delta\alpha$ may be required to compensate the camber force.

The mechanism of tyre distorsion is complex and it is expected that the longitudinal driving or braking force F_x gives rise to a change in ply-steer and thus in $\delta\alpha$. Firstly, through a direct change of the already present distorsion and secondly, through the creation of an additional angular distorsion as a result of F_x exerting a torque about the vertical axis. The torque arm arises due to lateral deformations caused by F_y and the camber angle γ.

This torque also contributes to the aligning torque M_z as will be shown later on. The total effective α-shift now becomes:

$$\delta\alpha = \delta\alpha_o + \delta\alpha_{Fx} \tag{13}$$

with $\delta\alpha_0$ the offset at pure side slip (possibly including camber) and $\delta\alpha_{Fx}$ the F_x-induced shift. The value of $\delta\alpha_0$ may be computed in an approximated way:

$$\delta\alpha_o = S_{hy} + S_{vy}/BCD_y \tag{14}$$

By introducing the torsional compliance c_{MFx} and the effective torsion arm a_{Fx}, the F_x-induced part of $\delta\alpha$ may be expressed as follows:

$$\delta\alpha_{Fx} = a_{Fx}.c_{MFx}.F_x + d_{Fx}.F_x \tag{15}$$

The Appendix shows the complete formula including the effects of F_y, γ and F_z. The values of the not yet known forces F_x and F_y may be approximated here by taking their values after one iteration step or through a simple approximate calculation [1] or by using their values from the preceding time step.

To account for the presence of the total composite slip, we may now replace the new absissas (12a,b) of the shifted two-sided characteristics for F_{x0} and F_{y0} (found at pure slip, indicated by the subscript o) by the total composite slip. We should, however, retain the sign of the slip components. The abscissas would then read $\sigma_{tot}\text{sgn}(\sigma_{x\,tot})$ and $\sigma_{tot}\text{sgn}(\sigma_{y\,tot})$ respectively.

It should be realized that by doing so, the two curves may reach their peak values at quite different values of σ_{tot}. This means that according to these new diagrams the state of complete sliding (which starts near the peak) would be reached at different values of composite slip. The tyre, however, will slip at one overall condition of sliding. This leads to the definition of the normalized composite slip σ^* with components

$$\sigma_x^* = \sigma_{xtot} / |\sigma_{xmtot}| \tag{16a}$$

$$\sigma_y^* = \sigma_{ytot} / |\sigma_{ymtot}| \tag{16b}$$

where the subscript m indicates the value of slip where the peak occurs. By using the normalized slip quantities, the rescaled characteristics F_{xo} and F_{yo} reach their peak values at normalized slip components with magnitude equal to unity. The thus established normalized characteristics will be used, but with the normalized composite slip σ^*, augumented with the signs of the slip components, as their abscissa.

The arguments which we will finally use for the normalized functions for F_{xo} and F_{yo} are $\sigma^*\text{sgn}(\sigma_x^*)$ and $\sigma^*\text{sgn}(\sigma_y^*)$ respectively. In

contrast to previous versions of the model, the complete double-sided pure slip characteristics are used. In Fig. 9 such a normalized characteristic has been shown.

It should be noted that, in general, we have a positive and a negative value of the slip components with subscript m where the peak occurs. The actual values of these quantities may be determined by performing one or two iteration steps to approximate the solution for x_m in Eq.(2). It might be better to provide already prepared approximate functions for x_m giving its relationship with F_z and γ.

A further problem which should be taken care of is the fact that different saturation levels in x and y directions may occur at large values of slip ($\mu_x \neq \mu_y$). It may be argued that at complete sliding of the tyre tread over the road surface, a single average friction coefficient arises which produces a resulting frictional force opposite to the average sliding speed (in approximate analytical studies taken equal to the slip speed V_s of the wheel).

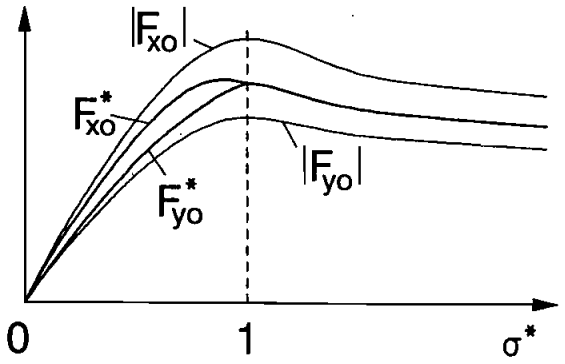

Fig. 6. Adopted normalized characteristics (shown for a given ratio σ_y^*/σ_x^*) from which the lateral and longitudinal force components are derived (cf. Fig. 7).

For this purpose, adapted normalized characteristics are used, which gradually deviate from the original curves until at $\sigma^* = 1$, a common curve is reached, situated in between the original curves (Fig. 6). The proportioning of the departures from the original curves is controlled by the ratio of the normalized slip components. The adapted normalized characteristics read:

$$F_{xo}^* = |F_{xo}| - \epsilon \left(|F_{xo}| - |F_{yo}| \right) (\sigma_y^*/\sigma^*)^2 \tag{17a}$$

$$F_{yo}^* = |F_{yo}| - \epsilon \left(|F_{yo}| - |F_{xo}| \right) (\sigma_x^*/\sigma^*)^2 \tag{17b}$$

with

$$\epsilon = \sigma^* \text{ for } \sigma^* \leq 1$$
$$\epsilon = 1 \text{ for } \sigma^* > 1$$

The composite shear force components are found by using a composite slip direction angle λ.

$$F_x = - F_{xo}^* \cos \lambda \cdot \operatorname{sgn} \sigma_x^* \tag{18a}$$

$$F_y = - F_{yo}^* \sin \lambda \tag{18b}$$

The composite slip direction varies from that of the normalized composite slip $\underline{\sigma}^*$ at small values of slip (almost complete adhesion where deformation slip prevails) to that of the original composite slip $\underline{\sigma}_{tot}$ at large values of slip. Figure 7 illustrates the process graphically. The following transition formula is used to determine λ:

$$\lambda = \eta + (\theta - \eta) \frac{\sin\{q_8 \arctan(q_9 \sigma^{*2})\}}{\sin(\tfrac{1}{2}\pi q_8)} \tag{19a}$$

with

$$\eta = \arcsin(\sigma_y^*/\sigma^*) \tag{19b}$$

$$\theta = \arcsin(\sigma_{y\,tot}/\sigma_{tot}) \tag{19c}$$

In Fig. 8 the variation of λ has been depicted for two values of the shape-factor q_8. This new formulation allows the direction angle λ (from which the direction of the force vector is derived) to surpass $\underline{\sigma}_{tot}$ before gradually turning back to the direction angle θ of $\underline{\sigma}_{tot}$. This possible course of λ may be made plausible as follows.

It is known that the torsion compliance of the lower part of the belt about the vertical axis reduces the cornering stiffness as a result of the action of the aligning torque M_z. In the range of larger slip this torque diminishes at increasing slip angle. It may even vanish and change its sign when the range of total sliding is entered. This phenomenon will be aggravated at combined slip. This entails that the cornering stiffness which is still felt at higher values of composite slip will be larger (because M_z is smaller) than at pure side slip. As a consequence, a smaller effective $|\sigma_{ym\,tot}|$ may result. Possibly even smaller than $|\sigma_{xm\,tot}|$ which would lead to an effective $|\eta| > |\theta|$. That would indeed cause an approach of the direction of $\underline{\sigma}_{tot}$ from the other side as illustrated in Fig. 8 at the larger value of the shape factor q_8.

Through the adapted formula for λ and the introduction of the F_x-induced α-shift (15), the correction quantities β and Ψ, used in the previous version [2], are no longer needed.

The aligning torque M_z is a complex result of the actions of F_y, F_x and a residual torque M_{zr}.

$$M_z = -tF_y + sF_x + M_{zr} \tag{20}$$

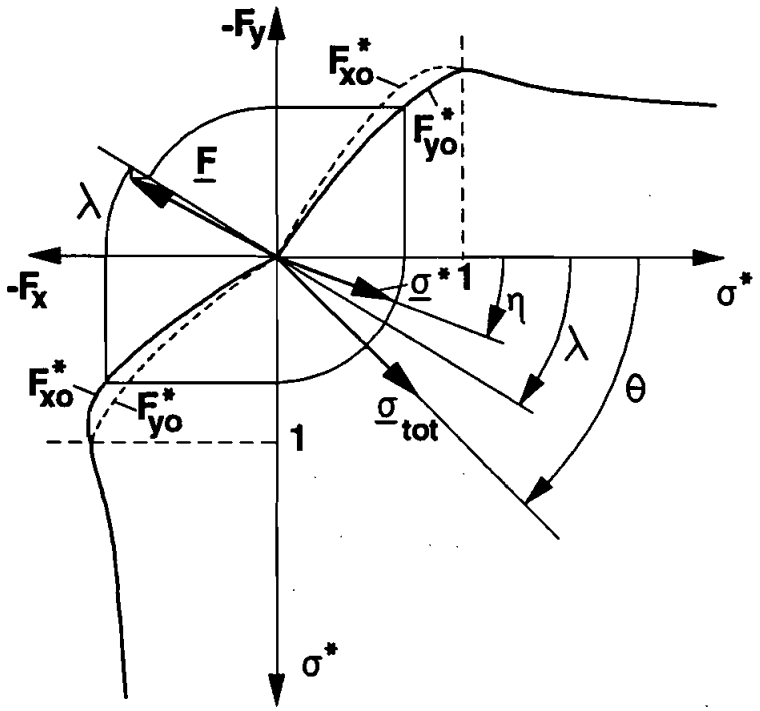

Fig. 7. Graphical illustration of the process to arrive at the force vector $\underline{F}$ starting out from the adapted normalized characteristics of Fig. 6 and using the composite slip direction angle λ.

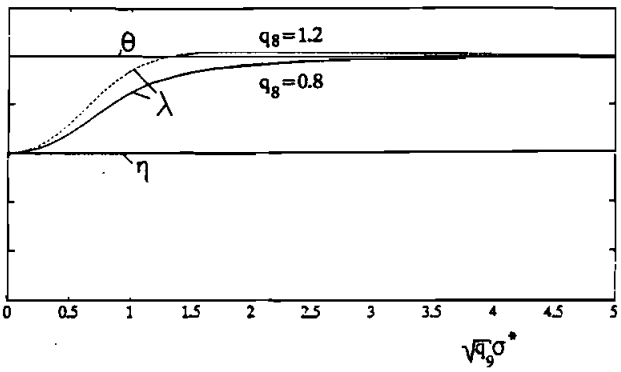

Fig. 8. Diagram showing possible courses of composite slip direction angle λ versus the magnitude of composite normalized slip σ^*, controlled by the parameters q_8 and q_9.

The offsets of the lines of action are t and s. The former is a function of σ^* and the latter depends on F_y and γ. The residual torque is considered to be the result of conicity and camber.

Figure 9 shows the characteristics for M_{zo} and F_{yo} as obtained from pure lateral slip measurements (hence subscript o). As abscissa is used the normalized lateral slip $-\sigma_y^*$ which for the purpose of considering combined slip may be replaced by $-\sigma^* \mathrm{sgn}(\sigma_y^*)$ as explained before.

To determine the pneumatic trail t, the aligning torque characteristic is first cleared from the residual torque M_{zr}. This torque is assumed to decay with increasing σ^*. The following formula is used

$$M_{zr}(\sigma^*) = \frac{M_{zro}}{1 + 5\sigma^{*2}} \tag{21}$$

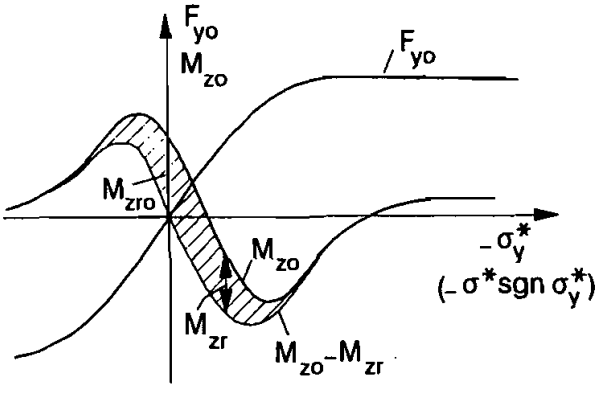

Fig. 9. Normalized characteristics for side force and aligning torque. The aligning torque contains the residual torque M_{zr}.

By subtracting M_{zr} from M_{zo} a curve is produced which together with F_{yo} passes through the origin. The pneumatic trail is now defined as the ratio of the remaining moment and the side force. As may be substantiated by analytical studies [6,7], t is assumed to vary with σ^* in the same way as it does with σ_y^* (pure side slip):

$$t(\sigma^*) = -\frac{M_{zo}(\sigma^*) - M_{zr}(\sigma^*)}{F_{yo}(\sigma^*)} \tag{22}$$

The reader is referred to the Appendix for more detailed formulae and the proper sequence of computation.

POSSIBLE ADDITIONS TO THE MODEL

Estimation of the possibly missing "driving" part of the longitudinal force characteristic

From the theory of an analytical tyre model (cf. [6,7 or 1]) it may be concluded that, at least for the case of dry friction, the F_x characteristic is anti-symmetric when plotted versus $\sigma_{x\,tot}$, i.e. $F(\sigma_{x\,tot}) = -F(-\sigma_{x\,tot})$. This anti-symmetry is lost when the function is plotted versus $\kappa + \delta\kappa$. The driving part of the characteristic may be artificially established by taking for σ_{tot} its opposite value when $\sigma_{x\,tot}$ becomes negative (i.e. at driving). With this opposite value we may then proceed to find κ (or κ' in case of combined slip, cf. Appendix). Then, the opposite value of the resulting F_x (or F_{xo}) should be taken to obtain the desired driving force.

Another way is to use the following quantity $\tilde{\kappa}$ as the argument of Y_x instead of κ (or κ'):

$$\tilde{\kappa} = \frac{\kappa - s.(1+\kappa).\delta\sigma_x}{1 + s.\{\kappa - (1+\kappa).\delta\sigma_x\}} - s.\delta\kappa \qquad (23)$$

where

$$s = 1 + \mathrm{sgn}(\kappa + \delta\kappa) = 1 - \mathrm{sgn}(\sigma_x^*)$$

$$\delta\sigma_x = \frac{-\delta\kappa}{1 - \delta\kappa}$$

In this latter method the anti-symmetry of the formula $Y(\kappa+\delta\kappa)$ is exploited ($\delta\kappa = S_{hx}$, $S_{vx} = 0$). It should be kept in mind that if the offset $\delta\kappa$ due to rolling resistance is to be included in the model, an additional rolling resistance torque

$$M_{yr} = -F_{xr}r_l \qquad (24)$$

should be applied to the wheel of the automobile simulation model. In (24) the rolling resistance force is denoted by $-F_{xr}$ which is found at $\kappa = 0$:

$$F_{xr} = Y_x(\kappa = 0) \quad (<0) \qquad (25)$$

The symbol r_l denotes the loaded radius.

Improvement of the aligning torque at combined slip

If at a given constant level of σ^* the lateral slip σ_y^* is varied from positive to negative values, the points of operation in the diagram of Fig. 9 jump from the left-hand side to the right-hand side of the diagram. Because of the asymmetry of the curve for M_{zo}-$M_{zr} = -tF_{yo}$ a discontinuity in the course of t vs α may occur which results in or

kink in the curve for the resulting M_z vs α at the point where $F_y = 0$. A special procedure may be used which averages and proportions the contributions to the variation of t due to lateral and longitudinal slip. A more appropriate course of M_z is established, but the computation time involved is considerable and we will not elaborate further on this procedure.

Running backwards or switching tyres from left to right side of a vehicle

When the direction of rolling is changed from forwards to backwards, which may be a result of switching the wheel from the left-hand side of the car to the right-hand side, the F_y and M_z characteristics may change with respect to measured data obtained at the left-hand position. At zero slip angle ($\alpha = 0$) a side force acts on the tyre which is composed of a ply-steer force and a conicity force. These forces are defined in such a way that the ply-steer force remains unaffected and that the conicity force changes its sign.

This characteristic of the tyre at the left-hand position should now be adapted to arrive at an estimate for the right-hand tyre. The difference seams to be twice the effect of the conicity. If the conicity force F_{yc} is known (from another special measurement) or assumed, an equivalent camber angle γ_{eq} may be defined. The mechanisms to generate side force and moment due to camber and conicity are similar. From additonal measurements involving camber, the camber stiffness $C_{F\gamma}$ may be derived. The resulting equivalent camber now reads:

$$\gamma_{eq} = \frac{F_{yc}}{C_{F\gamma}} \tag{26}$$

The estimated characteristic for the right-hand tyre follows by taking the model for the left-hand position but at a camber angle

$$\gamma = -2\gamma_{eq} \tag{27}$$

The proposed method may be liable for improvement. Experimental verification has not been conducted.

REFERENCES

1. H.B. Pacejka and R.S. Sharp, "Shear force development by pneumatic tyres in steady state conditions: A review of modelling aspects". Vehicle System Dynamics, 20 (1991), pp. 121-176.

2. E. Bakker, H.B. Pacejka and L. Lidner, "A new tire model with an application in vehicle dynamics studies". 4th Autotechnologies Conference, Monte Carlo, 1989. SAE 890087, pp. 83-95.

3. J. van Oosten and E. Bakker, "Determination of Magic Formula tyre model parameters". This issue.

4. L. Lidner, "Experiences with the Magic Formula tire model". This issue.

5. D. Schuring, private communication.

6. H.B. Pacejka, "Analysis of tire properties". Chapter 9, Mechanics of Pneumatic Tires (ed. S.K. Clark) DOT HS-805952, 1981, pp. 721-870.

7. H.B. Pacejka, "Modelling of the pneumatic tyre and its impact on vehicle dynamic behaviour". CCG course, Oberpfaffenhofen 1989.

APPENDIX
Formulae of the Magic Formula Tyre Model

GENERAL FORMULA FOR PURE SLIP

$$y(x) = D \sin[C \arctan\{Bx - E(Bx - \arctan(Bx))\}]$$

$$Y(X) = y(x) + S_v$$
$$x = X + S_h$$

B = stiffness factor
C = shape factor
D = peak factor
E = curvature factor
S_h = horizontal shift
S_v = vertical shift

$$D = y_{max}$$

$$C = 2/\pi \arcsin[y_s/D]$$

$$B = dy/dx_{(x=0)}/CD$$

$$E = (Bx_m - \tan(\pi/2C)) / (Bx_m - \arctan(Bx_m))$$

THE LATERAL FORCE

$Y_y = F_y$ (pure) or F_{y0} (combined)
$X_y = \alpha$ (pure) or α' (combined)

$$D_y = \mu_y F_z$$

$$\mu_y = (a_1 F_z + a_2)(1 - a_{15}\gamma^2)$$

$$BCD_y = a_3 \sin(2 \arctan(F_z/a_4))(1-a_5|\gamma|)$$

$$C_y = a_0$$

$$E_y = (a_6 F_z + a_7)(1 - (a_{16}\gamma + a_{17}) \operatorname{sgn}(\alpha+S_{hy}))$$

$$B_y = BCD_y / C_y D_y$$

$$S_{hy} = a_8 F_z + a_9 + a_{10}\gamma$$

$$S_{vy} = a_{11} F_z + a_{12} + (a_{13} F_z^2 + a_{14} F_z)\gamma$$

THE LONGITUDINAL FORCE

$Y_x = F_x$ (pure) or F_{x0} (combined)
$X_x = \kappa$ (pure) or κ' (combined)

$$D_x = \mu_x F_z$$

$$\mu_x = b_1 F_z + b_2$$

$$BCD_x = (b_3 F_z^2 + b_4 F_z) \exp(-b_5 F_z)$$

$$C_x = b_0$$

$$E_x = (b_6 F_z^2 + b_7 F_z + b_8)(1 - b_{13}\, \mathrm{sgn}(\kappa + S_{hx}))$$

$$B_x = BCD_x / C_x D_x$$

$$S_{hx} = b_9 F_z + b_{10}$$

$$S_{vx} = b_{11} F_z + b_{12}$$

If only brake forces available:
$b_{11} = b_{12} = b_{13} = 0$

THE SELF ALIGNING TORQUE

$Y_z = M_z$ (pure) or M_{z0} (combined)
$X_z = \alpha$ (pure) or α' (combined)

$$D_z = (c_1 F_z^2 + c_2 F_z)(1 - c_{18}\gamma^2)$$

$$BCD_z = (c_3 F_z^2 + c_4 F_z)(1 - c_6 |\gamma|) \exp(-c_5 F_z)$$

$$C_z = c_0$$

$$E_z = (c_7 F_z^2 + c_8 F_z + c_9)(1 - (c_{19}\gamma + c_{20}) * \mathrm{sgn}(\alpha + S_{hz})) / (1 - c_{10}|\gamma|)$$

$$B_z = BCD_z / C_z D_z$$

$$S_{hz} = c_{11} F_z + c_{12} + c_{13}\gamma$$

$$S_{vz} = c_{14} F_z + c_{15} + (c_{16} F_z^2 + c_{17} F_z)\gamma$$

COMBINED LATERAL AND LONGITUDINAL SLIP

$$\tan(\alpha) = -V_{sy}/V_x$$
$$\kappa = -V_{sx}/V_x$$
$$V_r = V_x - V_{sx}$$

$$\sigma_x = V_{sx}/V_r = -\kappa/(1+\kappa)$$
$$\sigma_y = V_{sy}/V_r = -\tan(\alpha)/(1+\kappa)$$

$$\delta\alpha_{fx} = (q_2 F_y + (q_6 + q_7 F_z)\gamma + q_3)(q_4 + q_5 F_z) F_x + (q_1 + q_{10} F_z) F_x$$

$$\delta\alpha = S_{hy} + S_{vy}/BCD_y + \delta\alpha_{fx}$$

$$\delta V_{sy} = V_r \tan(-\delta\alpha)$$
$$\delta\sigma_y = \delta V_{sy}/V_r = \tan(-\delta\alpha)$$
$$V_{sytot} = V_{sy} + \delta V_{sy}$$

$$\delta\kappa = S_{hx} + S_{vx}/BCD_x$$

$$\delta V_{sx} = V_r(-\delta\kappa/(1-\delta\kappa))$$
$$\delta\sigma_x = \delta V_{sx}/V_r = -\delta\kappa/(1-\delta\kappa)$$
$$V_{sxtot} = V_{sx} + \delta V_{sx}$$

$$\sigma_{xtot} = \sigma_x + \delta\sigma_x$$
$$\sigma_{ytot} = \sigma_y + \delta\sigma_y$$

$$\sigma_{x*}^{*} = \sigma_{xtot}/|\sigma_{xmtot}|$$
$$\sigma_y^{*} = \sigma_{ytot}/|\sigma_{ymtot}|$$

$$\sigma^{*} = \mathrm{sqrt}(\sigma_x^{*2} + \sigma_y^{*2})$$

$$F_{x0} = F_{x0}(\kappa') = Y_x(\kappa')$$
$$\kappa' = -\sigma_x'/(1+\sigma_x')$$

$$\sigma_x' = \sigma^{*}\sigma_{xmtot} - \delta\sigma_x$$

$$F_{y0} = F_{y0}(\alpha') = Y_y(\alpha')$$
$$\tan(\alpha')^{*} = -\sigma_y'$$
$$\sigma_y' = \sigma^{*}\sigma_{ymtot} - \delta\sigma_y$$

$$F_{x0*}^{*} = |F_{x0}| - \varepsilon(|F_{x0}| - |F_{y0}|)(\sigma_{y*}^{*}/\sigma^{*})^2$$
$$F_{y0}^{*} = |F_{y0}| - \varepsilon(|F_{y0}| - |F_{x0}|)(\sigma_x^{*}/\sigma^{*})^2$$

$$\varepsilon = |\sigma^{*}| \quad \text{for } \sigma^{*}<1$$
$$\varepsilon = 1 \quad \text{for } \sigma^{*}>1$$

$$\lambda = \eta + (\Theta-\eta)\sin(q_8 \arctan(q_9\sigma^{*2}))/\sin(\tfrac{1}{2}\pi q_8)$$

$$\eta = \arcsin(\sigma_y^{*}/\sigma^{*})$$
$$\Theta = \arcsin(\sigma_{ytot}/\sigma_{tot})$$

$$F_x = -F_{x0*}^{*}\cos(\lambda)\,\mathrm{sign}(\sigma_x^{*})$$
$$F_y = -F_{y0}^{*}\sin(\lambda)$$

$$M_{zr} = M_{zr0}/(1 + 5\sigma^{*2})$$
$$M_{z0} = M_{z0}(\alpha') = Y_z(\alpha')$$

$$t = t(\alpha') = -(M_{z0} - M_{zr})/F_{y0}$$
$$M_z' = -tF_y + M_{zr}$$

$$M_z = M_z' + (q_2F_y + (q_6 + q_7F_z)\gamma + q_3)F_x$$